SST Workshop, Tokyo, 3-5 December 2001

Boundary layer transition analysis on NEXST-1 airplane: NAL-ONERA cooperative research project

K. Yoshida, Y. Ueda, H. Sugiura, N. Tokugawa, T. Atobe
NATIONAL AEROSPACE LABORATORY
7-44-1 Jindaiji-higashi, Chofu,Tokyo, 182-8522, Japan
and
D. Arnal, J.P. Archambaud, A. Seraudie
ONERA /DMAE
2 avenue Edouard Belin – 31055 Toulouse Cedex 4 – France

Abstract

In the aerodynamic design of the National EXperimental Supersonic Transport (NEXST) program, a supersonic natural laminar flow (NLF) wing design concept was originally developed. Before the flight test of the NEXST-1 airplane, more detailed transition analysis should be performed in order to validate the NLF wing effect. Therefore, the NAL-ONERA cooperative research project started in April 2000, because ONERA had great ability of analyzing transition phenomena and NAL had some experimental transition data in supersonic flow. In the transition analysis on the sharp cone with a half angle of 5 degrees, the nose cone, and the NLF wing of the NEXST-1 airplane, almost good cross validation of both ONERA's and NAL's e^N codes was obtained. Then, there was also high correlation between the S2MA wind tunnel test results and both laboratories' predictions under the assumption of a critical transition N value of 6. Moreover, about 40% chordwise region was estimated to be laminar at flight condition by NAL's code. In addition, a risk of transition due to attachment-line contamination was predicted at inner wing, using the well-known Poll's criterion.

1. Introduction

The National Aerospace Laboratory (NAL) is promoting the National EXperimental Supersonic Transport (NEXST) program in Japan[1)]. In this NEXST program, two kinds of unmanned, scaled supersonic experimental airplanes have been designed and developed with an original CFD-based optimum aerodynamic design method. The first airplane, called the "NEXST-1" airplane, is a non-powered vehicle that has no propulsion system. Its flight test will be planned in June 2002, in order to validate the design method purely from the aerodynamic viewpoint. The second airplane, called the "NEXST-2" airplane, is a jet-powered vehicle. Its flight test will be planned in 2005 in order to establish the design method from the standpoint of applying the methodology to real aircraft design.

In the aerodynamic design of the NEXST-1 airplane, a design concept for the supersonic natural laminar flow (NLF) wing was originally developed and applied. The NLF wing design procedure was derived using two principles. The first involves stability analysis of transition characteristics of three-dimensional boundary layer on a highly swept wing[2)]. The second focuses on developing an effective CFD-based inverse design methodology[3)]. In general, transition prediction of boundary layer is one of the most difficult themes in modern aerodynamics. A current e^N method is well known as one of the effective methods in predicting transition qualitatively. The SALLY code[4)], which was one of the most popular e^N codes, was used in the NEXST-1 airplane design[5-6)]. However, the SALLY code was formulated by utilizing the incompressible stability theory. Before the flight test of the

NEXST-1 airplane, more detailed transition analysis with compressible effect should be performed. Also experimental validation should be conducted.

ONERA has been challenging transition prediction problem long time and developed some effective transition prediction methods[7]. One of the methods is a current e^N method. This method consists of boundary layer stability computations and estimation of so-called N factor. The stability computation derives eigenvalues of stability equations corresponding to amplification rates of small disturbances. The N factor is defined by integrating the amplification rates with some strategies. This method is well validated at both low speed and transonic speed through comparing predictions with experiments[7]. Presently its validity at supersonic speed has been investigated actively.

On the other hand, NAL has also recently developed a similar transition prediction tool but has not enough validation in supersonic flow yet[8]. Moreover NAL has already conducted some transition measurement tests in supersonic flow to investigate the effect of the NLF wing design concept[9]. Therefore, the NAL-ONERA cooperative research project started in April 2000 under the framework of some research activities in the NEXST program. The first objective has been a cross validation of each transition prediction tool in order to verify that both tools produce similar results in the analysis of real aircraft design. The second objective has been to develop a reliable database on the critical N values corresponding to natural transition.

While those transition measurement tests confirmed the NLF effect qualitatively, it was difficult to confirm it quantitatively. This has been a difficulty, because freestream turbulence has always been the source for generating transition. Therefore, wind tunnel tests are not a reliable way to estimate transition location at flight condition. We believe the solutions to this problem are the following two approaches. The first approach is to develop a special supersonic wind tunnel with extremely low freestream turbulence level such as NASA Low Disturbance Supersonic Tunnel (LDST). However, it requires very large amount of cost. The second approach is to conduct numerical transition prediction using the most effective and reliable computation tool. This will enable us to predict transition at flight condition with high precision, and will ensure that the NLF design concept is completely valid. This then is the heart of the third objective of our joint project, to find the most effective and reliable calculation tools for the prediction of transition at flight condition.

In our research project, three typical kinds of configurations were chosen in analyzing transition characteristics. The first configuration is a sharp cone with a half angle of 5 degrees. This is one of the simplest shapes at supersonic speed, with a wealth of reliable experimental transition data already accumulated. The second configuration is a nose cone of the NEXST-1 airplane. This is also a simple shape with an axisymmetrical feature, however, little reliable experimental transition data exists on the effect of pressure gradient. The third configuration is the NLF wing of the NEXST-1 airplane. This is a much more complicated shape. Its transition analysis includes a variety of aspects, such as, an effective path for integrating amplification rates and attachment-line contamination.

The objective of the present paper is to summarize several results obtained in our research activity. This paper consists of three parts. The first part is a fundamental transition analysis on the sharp cone. It describes cross-validation of both e^N codes and transition N database based on comparing predicted outcomes and test results. The second part is a transition analysis on the NEXST-1 airplane configuration at wind tunnel test condition. Some comparisons of transition characteristics on the nose cone and NLF wing, and measurement results are shown. These also deal with the integral path subject. The third part concerns transition prediction on the NEXST-1 airplane at flight condition. Estimated transition characteristics on the NLF wing, including the attachment-line contamination

subject, are summarized. These results should be compared with flight test results in the near future.

2. Fundamental transition analysis on the sharp cone

The sharp cone with a half angle of 5 degrees is one of standard models in researching transition characteristics in supersonic flow. This is one of the primary reasons that the sharp cone was chosen as the subject for the first cross validation study of ONERA's and NAL's transition prediction tools. The transition analysis was conducted at flight condition of Mach 2 and unit Reynolds number 9 million. Experimental transition data reflecting wind tunnel tests and the actual flight tests are summarized in ref.10.

In order to predict transition characteristics, velocity and temperature profiles in the laminar boundary layer were estimated under the condition of a constant Mach number 1.941 along the cone surface. That reduced value was estimated by the small disturbance theory. ONERA relied upon analytical methodology, specifically, the self-similar solution. However, NAL calculated the profiles using a numerical method. It is a finite difference method and is called the TUF code[11], which was derived by Herring and Mellor.

Figure 1 shows a comparison of the laminar boundary layer profiles computed by ONERA and NAL. There was good agreement at the condition of Prandtl number 0.72. Figures 2(a) and 2(b) show N characteristics computed by ONERA and NAL. Horizontal axis is the Reynolds number based on a displacement thickness. Each N curve corresponds to the small disturbances amplified with each frequency. Both laboratories applied the envelope strategy[7] in estimating N factors. Again, a very good correlation was obtained.

In light of the fact that both ONERA's and NAL's methods produced results that were both similar and valid, NAL concluded that NAL's numerical methodology and its prediction code could be used in computing the N characteristics at other flight Mach number cases. Figure 3 shows two critical N values estimated by NAL. The first is corresponding to the onset of transition and the second is the end of transition. These are estimated by comparing predicted N characteristics with transition Reynolds numbers based on the actual flight test data[10]. The actual flight conditions were measured under an extremely small freestream turbulence level. These N curves mean useful criteria to predict natural onset and end of transition at flight test condition.

In addition, ONERA and NAL have some wind tunnel test data on the sharp cone. ONERA has already found the onset of transition N value of about 6 in the continuous-flow type supersonic wind tunnel in Modane (ONERA-S2MA), by comparing predicted N characteristics by ONERA with measured transition location. Transition was detected with infra-red thermography. NAL conducted a transition measurement test at Mach 1.2 condition using NAL's continuous-flow type transonic wind tunnel (NAL-TWT). It has two different freestream turbulence levels in two different test sections (#1 and #3). The #1 test section consists of perforated walls with relatively high freestream turbulence level of Cp_{rms}=1.03%. The #3 test section has slotted walls with relatively low freestream turbulence level of Cp_{rms}=0.34%. Transition location was measured with Preston tube technique. According to the comparison of test results at the #3 section and NAL's prediction results, it was found that N=7 and 8 were corresponding to the onset and end of transition at wind tunnel test conditions as shown in figure 3. Therefore, figure 3 constitutes a database of transition criterion on axisymmetric bodies.

As another validation case, NAL compared predicted unstable wave characteristics with experimental results[12]. These tests were conducted in NAL's small supersonic wind tunnel (NAL-SSWT) under the conditions of Mach 1.5 to 2.5 and low freestream turbulence level with Cp_{rms}=0.1%. One of their comparisons is demonstrated in figure 4. These

experimental results show sound pressure level (SPL) at two different test conditions, that is, natural transition and rough surface conditions. On the other hand, the predicted result indicates N curve at several frequency conditions. In order to compare it with their experiments, each vertical axis was approximately adjusted. As shown in figure 4, the characteristics of predicted result was in fairly good agreement with those of the experimental results.

Therefore, the present study on the sharp cone confirmed that both ONERA's and NAL's transition prediction tools yielded nearly identical results and their unstable wave characteristics also had good agreement with experimental results.

3. Transition analysis on the NEXST-1 airplane configuration at wind tunnel test condition

In general, most blow-down type supersonic wind tunnels do not have low freestream turbulence levels, hence it is not easy to obtain any precise transition data. To confirm the NLF wing effect experimentally, NAL chose two kinds of wind tunnels with relatively low freestream turbulence levels. One is the small in-draft type tunnel at Fuji Heavy Industries (FHI), the other is the large continuous circuit flow type tunnel at ONERA-S2MA. Through these test results, the NLF wing effect was confirmed qualitatively[9]. Once these tests were verified, comparisons of transition predictions and test results conducted at the S2MA were investigated.

In addtition, the transition characteristics on the nose cone of the NEXST-1 airplane were investigated in detail by both ONERA and NAL, because this configuration was chosen as a standard model to consider the relation between transition Reynolds numbers and freestream turbulence levels. Especially, useful transition measurement data with three kinds of turbulence levels were obtained at M=1.2 case, using NAL-TWT(#1 and #3 carts) and S2MA. The main results are summarized as follows.

3-1. The nose cone of the NEXST-1 airplane

The nose cone was designed by applying a part of the Sears-Haack body to a straight fuselage in order to reduce wave drag due to the volume of the NEXST-1 airplane. Precisely speaking, the Sears-Haack body has a blunt nose and tail. Employing a blunt nose leads to a detached shock wave in front of the nose. Therefore, pressure distribution along the nose surface was estimated by NAL's Euler code at conditions of M=1.2 and M=2.0 respectively.

However, a small approximation near the nose, that is, removing the rapid pressure rise due to the detached shock wave was applied, because no rapid pressure rise was necessary to compute laminar boundary layer. In addition, it is very important to specify the upstream condition carefully, taking account of influence of the detached shock wave. This means reducing the total pressure at the upstream condition after the shock wave. Then ONERA and NAL predicted transition characteristics using those approximated pressure distributions and upstream conditions.

Figure 5 shows a summary of NAL's transition measurement test results. They were conducted at Mach 1.2 under the different freestream turbulence levels (Cp_{rms}=0.34%,1.03% and 2.25%), which were measured at three different test sections (#1 and #3 carts) of NAL-TWT and ONERA-S2MA tunnel. The transition locations were detected with a hot-film sensor. In this figure, dashed horizontal lines are transition Reynolds numbers corresponding to the onset of transition.

Figures 6(a) and 6(b) show the comparison of the estimated N characteristics by ONERA and NAL at the NAL-TWT test condition of Mach 1.2. There is very good agreement between both N characteristics. Also comparing them with the test results, the

transition N values of 4.0 and 5.8 due to the onset of transition were obtained at the two different turbulence levels of NAL-TWT tests. However, if the transition N criterion of N=4.8 and 7 based on the sharp cone test by NAL (see figure 3) was applied, a remarkable difference of about 1 was detected between them. This is different from our expectation that the transition N criterion on the sharp cone is applicable to predicting transition locations on any axisymmetrical bodies.

Figures 7(a) and 7(b) also show the similar comparison at Mach 2.0 condition. The envelopes of both ONERA's and NAL's N curves are nearly the same. However, there is small difference in each N curve with the same frequency. It is supposed that the main reason for these differences originate in non-dimensionalizing frequency. Moreover, there is a larger difference between the transition N value of about 3.5 at the onset of the transition and the N-criterion of N=6, which was based on the sharp cone test at S2MA tunnel by ONERA. Any clear solution for those discrepancies has not been found yet. As we all know, it is not easy to analyze transition characteristics of any axisymmetrical bodies with a blunt nose. Further study is necessary to investigate the discrepancy in detail.

3-2. The NLF wing of the NEXST-1 airplane

Before mentioning the present transition analysis results on the NLF wing of the NEXST-1 airplane, a brief summary of the transition measurement tests at the S2MA tunnel is demonstrated in figure 8. In the test, transition locations were measured by using hot-film sensors and infra-red (IR) camera techniques. Based on the summary of the IR test results shown in the figure, rearward movement of the transition location was clearly obtained at the design point. However, the amount of laminar region was not always similar to the predicted region by NAL at flight test condition, because there were differences in the unit Reynolds number and freestream turbulence level. Therefore, our NLF wing design concept was not quantitatively but qualitatively validated.

In order to perform the transition analysis, compressible laminar boundary layer profiles were estimated. ONERA used an in-house code called 3C3D and NAL used the popular code developed by Kaups & Cebeci[13]. First of all, NAL compared both estimated boundary layer thickness distributions, and naturally found very good agreement.

While each e^N method has the same envelope strategy[7], each is based upon a different formulation of the integral path of amplification rates. As we all know, the selection of the best integral path is an open question. As a candidate, a path along a polar arc, which was indicated by "path A" in figure 9, was naturally selected by ONERA, because both 3C3D method and the Kaups & Cebeci method were formulated in the polar coordinate (x_c, z_c) system. On the other hand, NAL considered two candidates of the path in order to investigate the ideal integral path for practical applications. One is the same as ONERA's path. The second is a path along a local streamline, which we called "path B" as demonstrated in figure 9. This selection was based on the fact that NAL's stability code was formulated in the local streamline coordinate (x_s, z_s) system. Previously, there had been no investigation of the differences between these two proposed paths. Therefore, NAL investigated both proposed paths to assess their reliability.

A comparison of ONERA's and NAL's N characteristics at the S2MA test condition with a stagnation pressure of 0.6 bar, which was conducted by NAL, is shown in figures 10(a), 10(b) and 10(c). In this comparison, both ONERA and NAL calculated the N curves using the integral path A (see figures 10(a) and 10(b)). At this relatively low stagnation pressure case, the N evolution was quite similar except the rearward chordwise region. However, NAL's computation with the integral path A produced slightly lower N factors than ONERA's. Moreover, NAL's N factors, computed on the integral path B (see figure 10(c)), were found to be about 0.3 less than the path A. A comparison of the S2MA test results[9] and both

computations demonstrates that the result was N=5.4 in ONERA's case, while NAL's results were estimated at N=4.7 and 4.4 for the path A and B respectively. If a transition N criterion of N=6 is assumed, it is found that ONERA's prediction has a better correlation with the S2MA test result than the NAL's prediction.

As above mentioned, the N=6 criterion for the onset of transition on the sharp cone case was experimentally obtained by ONERA at S2MA tunnel test condition. This criterion is related to the transition dominated by T-S instability. The T-S instability is also dominant in our NLF wing case, because the C-F instability, which is generated at highly swept wing, is suppressed by applying our NLF wing design concept. Therefore, ONERA's high correlation between the test result and computation is well understandable. On the other hand, both NAL's estimated transition N factors are less than the N=6 criterion. One of the main reasons for such a difference certainly depends on the integral path. However, no clear solution for the path A case has been found yet.

In addition, NAL's estimated propagation direction of small disturbances was very similar to ONERA's result, as shown in figures 11(a) and 11(b). This means that the real part of eigenvalue estimated by ONERA and NAL is very similar, as easily supposed by the high correlation between ONERA's and NAL's computation results for the sharp cone case.

Similar comparisons at 70% semi-spanwise station and a relatively high stagnation pressure of 1.4 bar condition are summarized in Table 1. In the case of 70% semi-spanwise station at 0.6 bar, both ONERA's and NAL's N characteristics were also similar, but they were much less than the N=6 criterion. It is supposed that this discrepancy is due to the difference between measured and calculated pressure distributions. However, any clear solution for this discrepancy has not been found yet. In the case of 1.4 bar, there were also similar N evolutions. In these cases, ONERA's predictions have high correlation with the N=6 criterion. As a conclusion, there is good agreement between test results and ONERA's predictions under the assumption of applying the N=6 criterion on the sharp cone into the NLF wing test case. Only exception is the prediction in the case of 70% semi-spanwise station at 0.6 bar.

As mentioned above, NAL's predictions with the integral path A or path B were much less than the N=6 criterion. Therefore, another e^N method with a different path model, which was originally derived by Itoh[14], was applied to present NLF wing case by NAL. This method consists of estimating eigenvalues by using usual linear stability method and calculating N factors by applying a complex ray theory. The complex ray theory leads to one necessary condition to select a unique and meaningful propagation path for small disturbances. The detail is described in ref. 14.

Figure 12 shows a comparison of N curves corresponding to the special frequency of 10 kHz at 30% semi-spanwise station in the case of 0.6 bar test condition. New result, which is indicated by "ATOBE", is more similar to NAL's result with the path B ("LSTAB") than ONERA's result, because the same laminar boundary layer profiles by NAL were used. However, there was remarkable difference in aft-chord region. It reflects the difference of the integral path. Qualitative trend of the N evolution is rather similar to the ONERA's result. However, in order to predict the transition location comparing with the N =6 criterion, several N curves corresponding to several frequencies must be estimated. NAL has been conducting this work. In the near future, the detail will be published as a NAL technical report[15].

4. Transition prediction on the NEXST-1 airplane configuration at flight test condition

According to present relatively high correlation in both e^N codes, the transition characteristics of the NEXST-1 airplane at flight condition were predicted by using NAL's code and summarized in figure 13. The assumption of the "integral path B" was used in the

prediction, because this model was more reasonable in NAL's stability formulation. However, it produced relatively lower N factors than ONERA's predictions. The difference is about 1, as mentioned above. If N=14 is chosen as a transition N value based on the NASA's wind tunnel test result, large laminar region from the leading edge to about 40% chordwise location would be expected at the design point of flight condition. The difference of the N factor of about 1 shows no remarkable difference of transition characteristics. Although this region is smaller than the result estimated at design process, it is much larger than conventional region of usual supersonic airplanes. The result will be validated in the flight test planned in June 2002.

Figure 14 shows the N characteristics on the nose cone at flight test condition estimated by ONERA (dotted lines) and NAL (solid lines). Although there is a slight difference between them as similar to the M=2 case in S2MA, both envelopes of the N curves are nearly the same. Referring to the results in figure 3, if N=17 is assumed as a transition N value for the axisymmetric bodies at flight condition in spite of relatively lower unit Reynolds number, it is expected that no transition due to T-S instability is generated before the location of 26% of the fuselage length, which is approximately corresponding to the station of wing-body junction. Also this result will be investigated in the flight test.

In a swept wing, it is well known that there is another transition mechanism, which is different from the transition due to T-S and C-F instability. This is the transition due to attachment-line contamination originated in a turbulent boundary layer on the fuselage surface[7]. Although this process cannot be analyzed theoretically, it is well known that Poll's criterion[16] based on empirical database is very effective as a practical tool. Therefore ONERA and NAL applied the criterion to the NLF wing case.

Poll's criterion indicates that there is no risk of transition due to attachment-line contamination, if the special Reynolds number $\overline{R}^*$ is less than 245 ± 35. In general, the $\overline{R}^*$ is related to the boundary layer characteristics of attachment-line flow, compressibility effect and curvature radius of the leading edge. It is a main job to estimate $\overline{R}^*$ in this subject. ONERA and NAL used the exact definition of $\overline{R}^*$ demonstrated in figure 15(a). The most important point is to calculate velocity (Ue) gradient at the attachment-line. There are two approaches to estimate the velocity gradient. One is to apply the infinite swept wing assumption to the pressure distribution calculated by NAL's NS solver with standard grid. Another is to estimate the velocity (Ue) distribution directly using NAL's NS solver with much more fine grid system and all laminar boundary layer condition. The former was used by ONERA, and the latter was used by NAL.

Figures 15(a) and 15(b) show the velocity distributions on surface at the plane normal to the leading edge. ONERA's and NAL's estimated velocity distributions are nearly the same. (It is necessary to notice that the horizontal axis in ONERA's computations is 0.233 times in NAL's ones.) Figure 16 shows estimated $\overline{R}^*$, comparing ONERA's and NAL's results. It was found that there was almost good correlation between both results. If the Poll's criterion is valid, it is supposed that there is a risk of transition due to attachment-line contamination, at inner wing region. However, this study should be investigated more precisely, because this result strongly depends on the precision of calculating the velocity gradient at attachment-line. This is one of future work to be studied.

5. Concluding remarks

In the analysis on the sharp cone, the nose cone, and the NLF wing of the NEXST-1 airplane, almost good cross validation of both ONERA's and NAL's stability codes was obtained. Then, at the S2MA wind tunnel test condition, there was also high correlation

between the test results and the predictions under the assumption of a critical transition N value of 6. According to present good validation of NAL's transition prediction tool, about 40% chordwise region was estimated to be laminar at flight condition by NAL's code. In addition, a risk of transition due to attachment-line contamination was predicted at inner wing using Poll's criterion.

References

1. Sakata, K., "SST Research Project at NAL", 1st International CFD Workshop on Supersonic Transport Design, Tokyo, March, pp.1-4, 1998
2. Ogoshi, H., "Aerodynamic Design of an Supersonic Airplane Wing – Application of the Natural Laminar Flow Concept to Airfoil", Proc. of the 47th Nat. Cong. of Theoretical & Applied Mechanics, Jan., 1998 (in Japanese)
3. Matsushima, K., Iwamiya, T., Jeong, S. and Obayashi, S., "Aerodynamic Wing Design for NAL's SST Using Iterative Inverse Approach", 1st International CFD Workshop on Supersonic Transport Design, Tokyo, March, pp.73-78, 1998
4. Srokowski, A.J., "Mass Flow Requirement for LFC Wing Design", AIAA-77-1222, 1977
5. Yoshida, K., "Overview of NAL's Program Including the Aerodynamic Design of the Scaled Supersonic Aircraft", held at the VKI, RTO Educational Notes 4, 15-1~16, 1998
6. Shimbo, Y., Yoshida, K., Iwamiya, T., Takaki, R. and Matsushima, K., "Aerodynamic Design of the Scaled Supersonic Experimental Airplane", 1st International CFD Workshop on Supersonic Transport Design, Tokyo, March, pp.62-67, 1998
7. Arnal, D., "Boundary layer transition: prediction based on linear theory", AGARD FDP/VKI Special Course on Progress in Transition Modeling, AGARD Report 793, 1993
8. Yoshida, K., Ishida, Y., Noguchi, M., Ogoshi, H. and Inagaki, K., "Experimental and Numerical Analysis of Laminar Flow Control at Mach 1.4", AIAA Paper 99-3655, 1999
9. Sugiura, H., Yoshida, K., Tokugawa, N., Takagi, S. and Nishizawa, A., "Transition Measurements on the Natural Laminar Flow Wing at Mach 2", AIAA-2001-2782
10. Fisher, D. F. and Dougherty, N. S. Jr., "In-Flight Transition Measurement on a 10^{o} Cone at Mach Numbers From 0.5 to 2.0", NASA TP-1971, 1982
11. Herring, H. J. and Mellor, G. L., "Computer Program for Calculating Laminar and Turbulent Boundary Layer Development in Compressible Flow", NASA CR-2068
12. Okuwa, T., Tokugawa, N, Takagi, S., Yoshida, K. and Ueda, Y., "Prediction and validation of supersonic boundary layer transition on 10 degrees cone (in Japanese)", The 29th NAL Workshop on "Investigation and Control of Boundary-Layer Transition", will be published in March 2002.
13. Kaups, K. and Cebeci, T., "Compressible Laminar Boundary Layers with Suction on Swept and Tapered Wings", J. Aircraft, Vol.14, No.7, pp.661-667, 1977
14. Itoh, N., "Structure of Absolute Instability in 3-D Boundary Layers: Part 1. Mathematical Formulation", Trans. Japan Soc. Aero. Space Sci., Vol.44, No.144, pp.96-100, 2001
15. Atobe, T., "Transition Prediction of Boundary Layer in Supersonic Flow Using a Complex Ray Theory", NAL Technical Report, will be published in October 2002
16. Poll, D.I.A., "Boundary layer transition on the windward face of space shuttle during re-entry", AIAA paper 85-0899, 1995

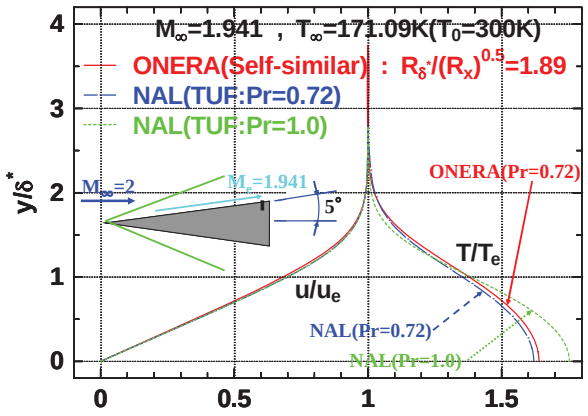

Figure 1. Laminar boundary layer profiles on the sharp cone

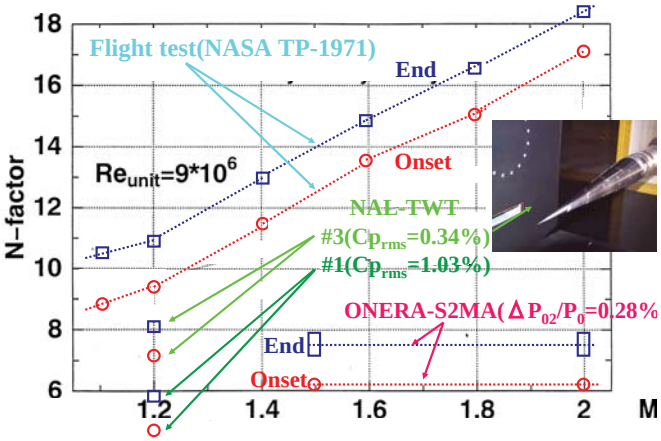

Figure 3. Transition N-criterion on the sharp cone, based on NAL's e^N code

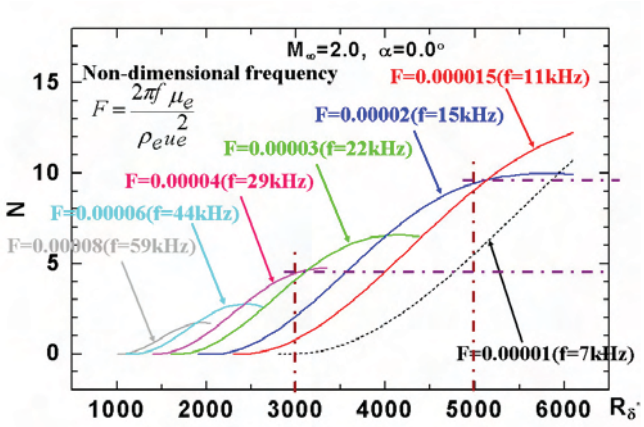

(a) ONERA's computations

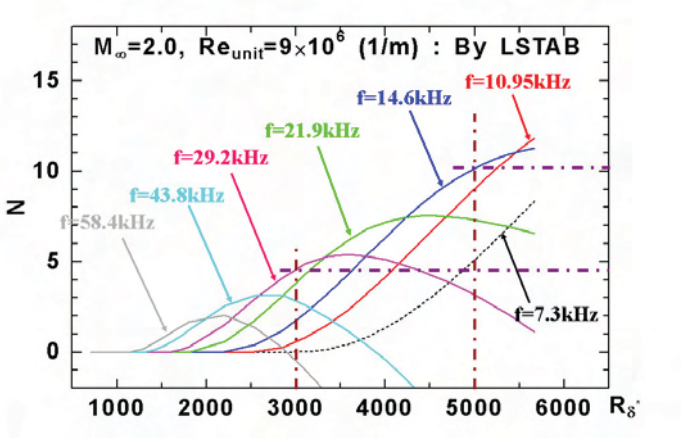

(b) NAL's computations

Figure 2. Comparison of estimated N-factors on the sharp cone

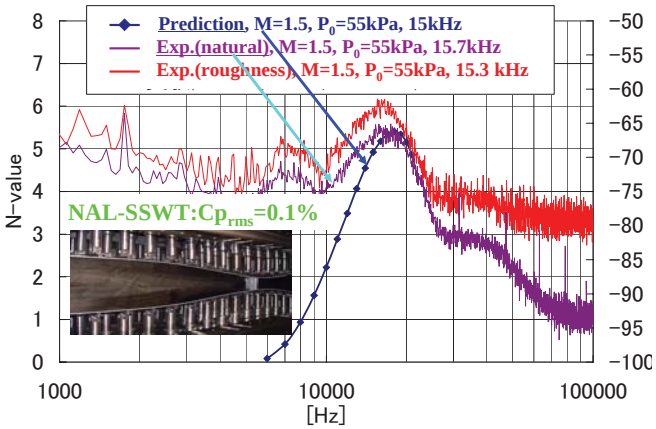

Figure 4. Unstable wave characteristics on the sharp cone

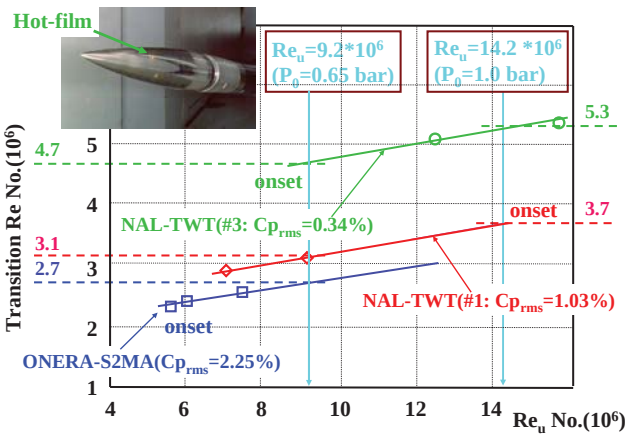

Figure 5. Transition test results on the nose cone at M=1.2

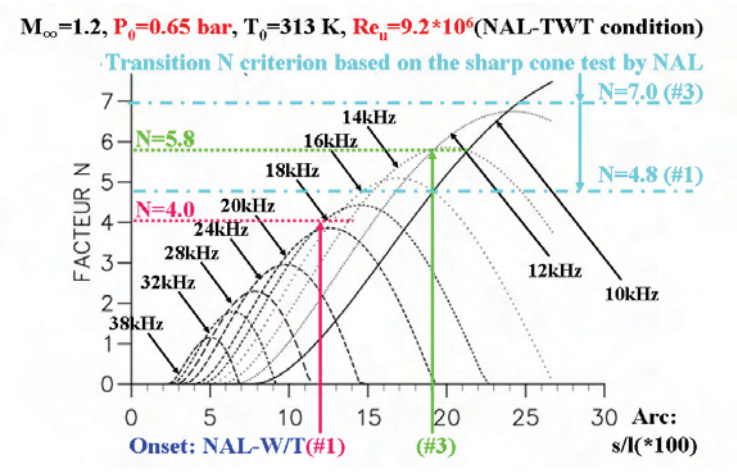

(a) ONERA's computations

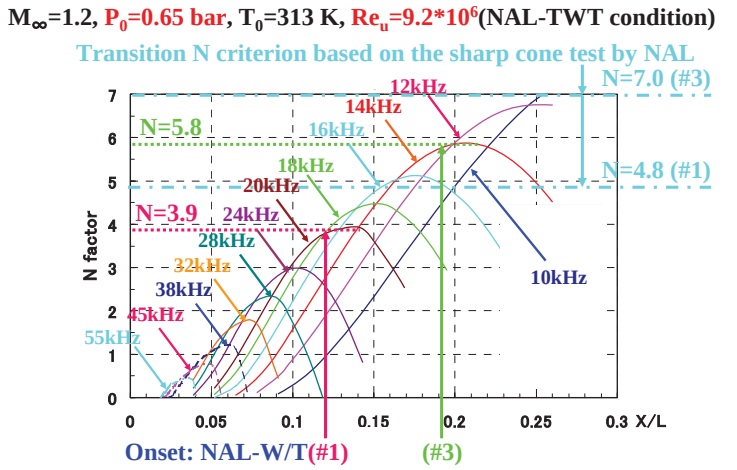

(b) NAL's computations

Figure 6. Comparison of N-factors on the nose cone at M=1.2

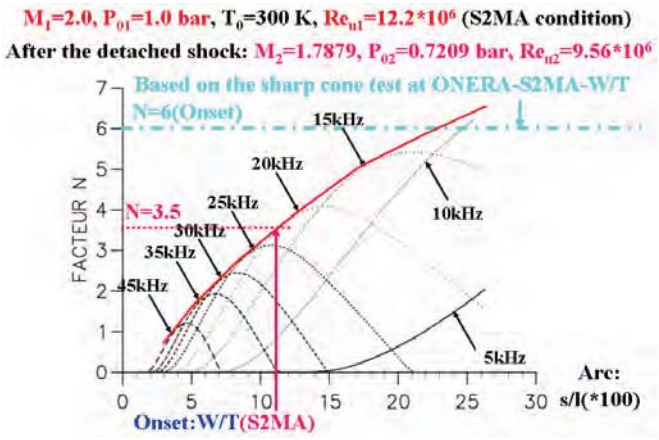

(a) ONERA's computations

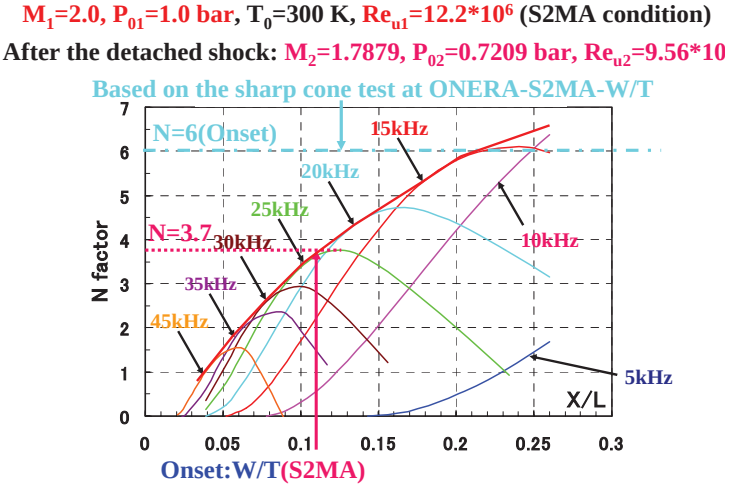

(b) NAL's computations

Figure 7. Comparison of N-factors on the nose cone at M=2.0

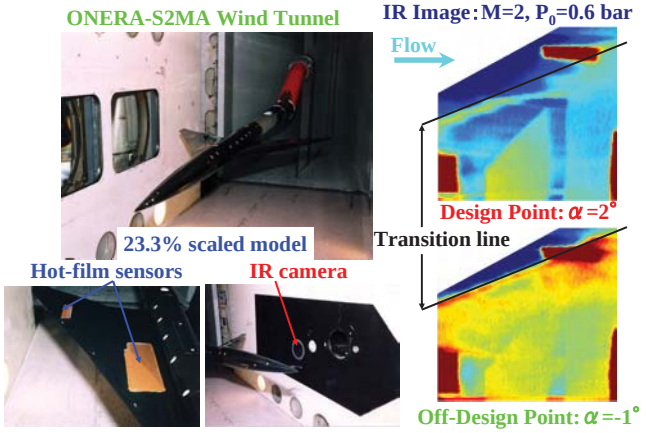

Figure 8. Transition measurement test of the NEXST-1wing

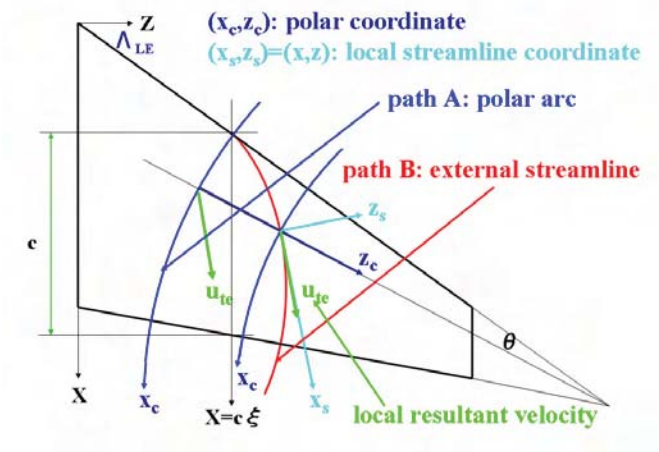

Figure 9. Typical candidates of integral path in stability analysis

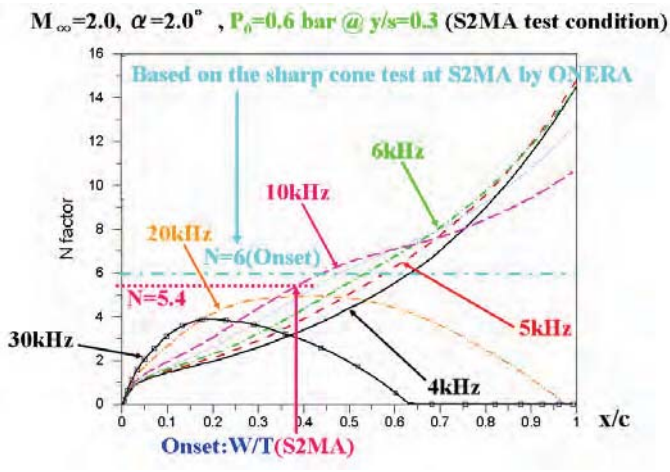

(a) ONERA's computations

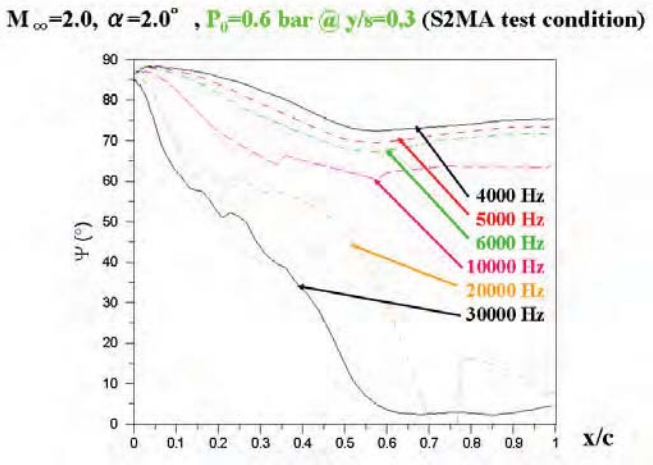

(a) ONERA's computations

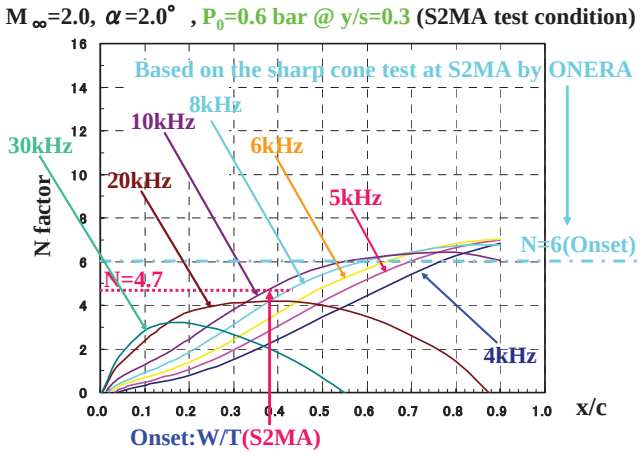

(b) NAL's computations with the integral path A

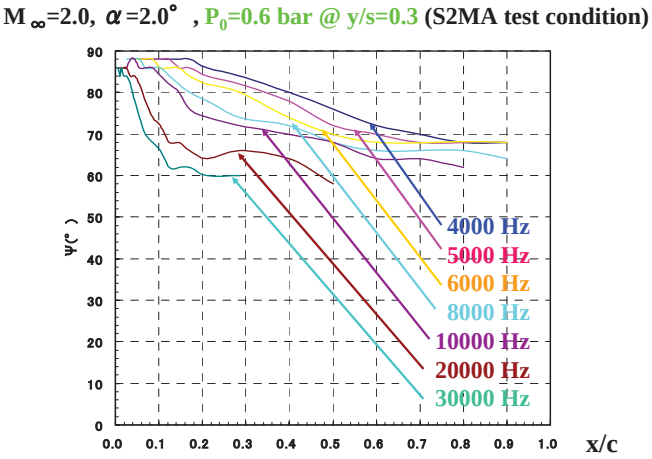

(b) NAL's computations

Figure 11. Comparison of N-factors on the NEXST-1 wing

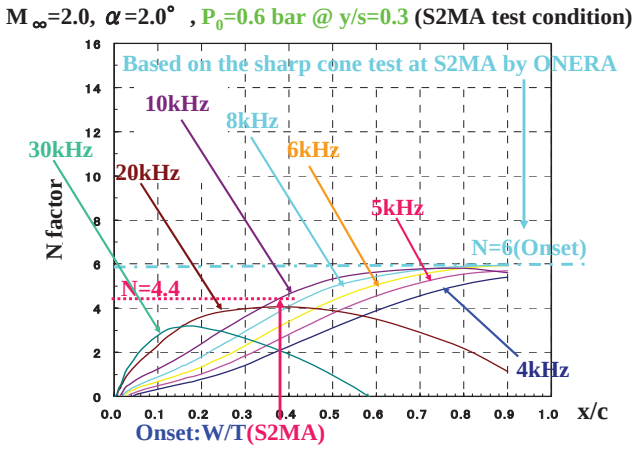

(c) NAL's computations with the integral path B

Figure 10. Comparison of N-factors on the NEXST-1 wing

Table 1. Comparison of ONERA's and NAL's N-factors on the NEXST-1 wing based on the S2MA test results

W/T			ONERA		NAL			
Cond.	HF Results		Path A		Path A		Path B	
P_0	y/s	$(x/c)_{Tr.}$	N_{onset}	f_{max}	N_{onset}	f_{max}	N_{onset}	f_{max}
0.6 bar	0.3	0.38	5.4	10kHz	4.7	10kHz	4.4	10kHz
	0.7	0.44	3.4	20kHz	3.1	20kHz	2.9	20kHz
1.4 bar	0.3	0.11	6.3	40kHz	5.2	30kHz	5.1	30kHz
	0.7	0.21	5.7	50kHz	4.5	50kHz	4.5	50kHz

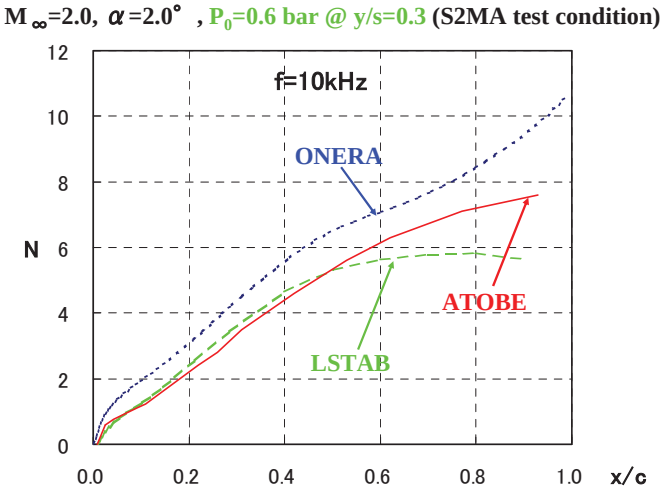

Figure 12. Comparison of three e^N methods

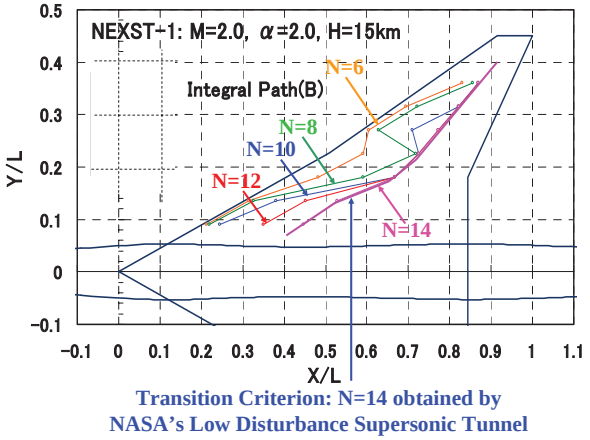

Figure 13. Transition predictions on the wing at flight condition

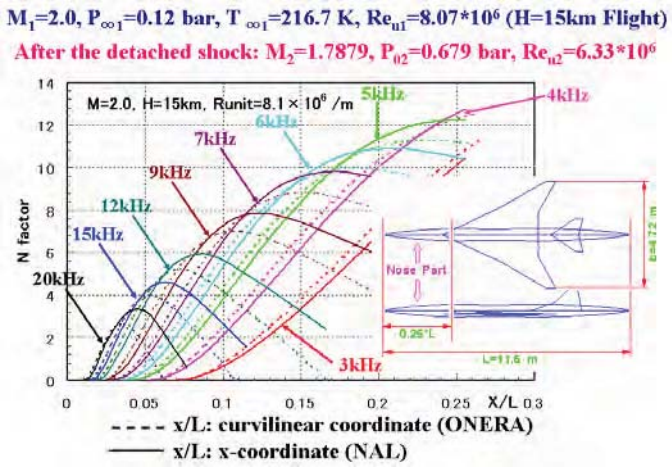

Figure 14. Transition predictions on the nose at flight condition

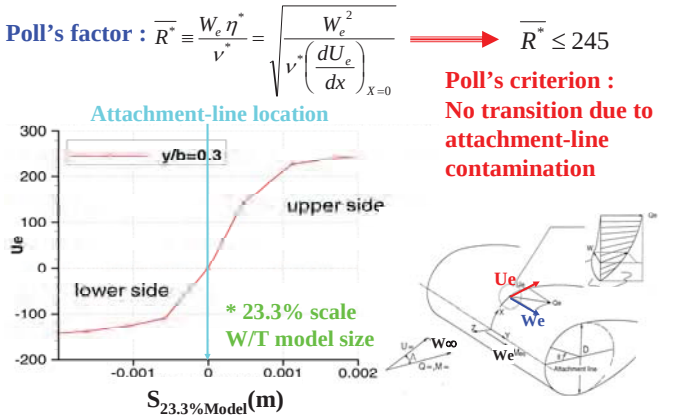

(a) ONERA's computation

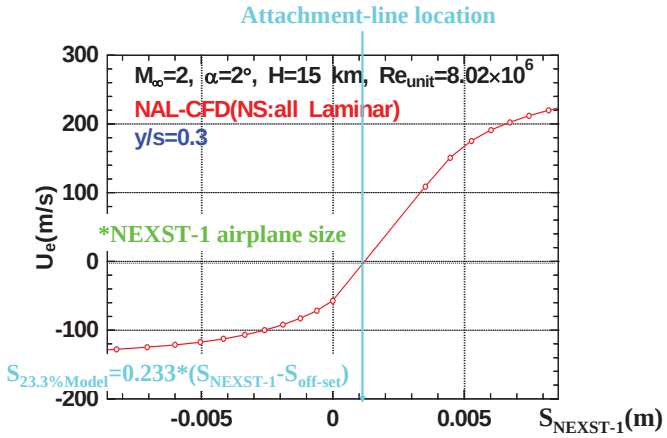

(b) NAL's computation

Figure 15. Normal velocity distribution near attachment-line

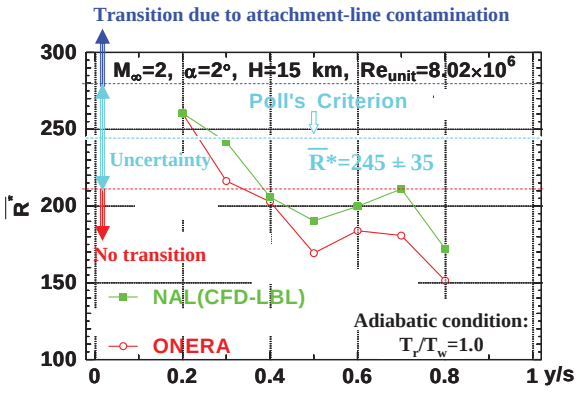

Figure 16. Analysis results on attachment-line contamination